AGU PUBLICATIONS

JGR

Journal of Geophysical Research: Atmospheres

RESEARCH ARTICLE

10.1002/2014JD021651

Key Points:
- The distribution of lightnings is affected by the location and storm intensity
- Over the open ocean, lightning activity is higher at higher storm intensity
- At TS stage, lightning activity increases before a rapid intensification

Correspondence to:
C. Bovalo,
christophebovalo@gmail.com

Citation:
Bovalo, C., C. Barthe, N. Yu, and N. Bègue (2014), Lightning activity within tropical cyclones in the South West Indian Ocean, *J. Geophys. Res. Atmos.*, *119*, 8231–8244, doi:10.1002/2014JD021651.

Received 15 FEB 2014
Accepted 7 JUN 2014
Accepted article online 11 JUN 2014
Published online 08 JUL 2014

Lightning activity within tropical cyclones in the South West Indian Ocean

C. Bovalo[1,2], C. Barthe[1], N. Yu[1], and N. Bègue[1]

[1]Laboratoire de l'Atmosphère et des Cyclones, UMR 8105 CNRS/Météo-France/Université de La Réunion, Sainte-Clotilde, France, [2]Now at Laboratoire d'Aérologie, UMR 5560, Université de Toulouse/CNRS, Toulouse, France

Abstract Lightning activity within 70 tropical cyclones in the South West Indian Ocean is studied using a large data set (2005–2013) provided by the World Wide Lightning Location Network (WWLLN). The radial and azimuthal distributions of lightning flashes are analyzed in three different regions of the basin: the open ocean, the Mozambique Channel, and the oceanic region up to 400 km off the eastern coast of Madagascar (ECM). Over the open ocean, lightning activity detected by the WWLLN is mainly found in the eyewall and decreases outward, regardless of storm intensity. Lightning activity in the eyewall of tropical cyclones is higher than in the eyewall of tropical storms. The front and the right quadrants (225° to 45°) relative to the storm motion are the regions where lightning flashes are preferentially detected. Near the ECM, lightning density in the eyewall, the inner rainbands, and the outer rainbands is quite similar, presumably owing to the proximity of land. When the system reaches tropical cyclone strength, lightning activity is mainly found in the left and rear quadrants relative to storm motion. In the Mozambique Channel, the radial and azimuthal distributions of lightning flashes are complex due to the geographical configuration of this subdomain. The relationships between lightning activity and intensity change have also been investigated for systems over the open ocean. The proportion of periods with lightning activity is higher during rapid intensity changes of tropical cyclones. During tropical storm stage, lightning activity in the outer rainbands starts increasing 18 h before a rapid intensification period.

1. Introduction

While tropical cyclone (TC) track forecasts have been improved for the past few decades (http://www.nhc.noaa.gov/verification/verify5.shtml), TC intensity forecasts, in particular, rapid intensity changes, are still a difficult task. *Black and Hallett* [1999] first suggested that lightning activity could be an indicator of TC intensity or track change. Analyzing the distribution of lightning flashes within TCs and determining its potential usefulness toward forecasting intensity change have been made increasingly possible owing to the development and improvement of lightning detection systems.

The National Lightning Detection Network (NLDN) primarily detects cloud-to-ground (CG) lightning strokes within 400 km of the United States coasts. TCs in this region start interacting with land and usually make landfall. *Samsury and Orville* [1994] studied the lightning activity in two Atlantic hurricanes using the NLDN. Hurricane Hugo (1989) only produced 33 CG strikes over an 18 h period with 17 flashes in and around the eyewall. Hurricane Jerry (1989), in contrast, generated a larger number of flashes (691). Lightning activity peaked when Jerry weakened from hurricane strength to tropical storm. Most of the CG strikes were located in the rainbands. For both hurricanes, lightning activity was mainly located in the right front and right rear quadrants. *Lyons and Keen* [1994] focused on four tropical cyclones (from tropical storm to hurricane stage). They found that lightning activity was more frequent in supercells in the outer rainbands and quite rare near the storm center. They also noticed that bursts of lightning activity near the storm center preceded periods of intensification in hurricanes Diana (1984) and Florence (1988).

Molinari et al. [1999] studied lightning activity in nine hurricanes of the Atlantic basin using data from the NLDN. They showed that lightning activity within tropical storms did not depend on the maximum intensity as hurricane Hugo (1989) had a very low flash rate while marginal hurricane Bob (1985) was the most electrically active hurricane with up to 5700 flashes d^{-1}. The main features of lightning distribution were (1) maximum of lightning activity in the rainbands (more than 200 km from the center), (2) a second moderate maximum near the storm center (less than 60 km), and (3) a gap near 80–100 km. They also found that

outbreaks of lightning flashes occurred before landfall, before the hurricane reached its maximum intensity, and during eyewall replacement cycles.

Corbosiero and Molinari [2003] studied the azimuthal distribution of lightning flashes detected by the NLDN, relative to storm motion and wind shear in 35 named tropical cyclones within 400 km of the U.S. coasts. They showed that the maximum of lightning activity was found in the front or right side of tropical cyclones for the inner core (0–100 km) and the rainband region (100–300 km). This general distribution was attributed to the asymmetric frictional force in the tropical cyclone boundary layer [*Shapiro*, 1983]. Moreover, they showed that the location of lightning activity also depended on the angle between the wind shear and motion vectors.

More recently, *Nagele* [2010] studied lightning activity detected by the NLDN within TCs of the Atlantic basin. She focused on the spatial and temporal distribution of lightning flashes within TCs that made landfall. Her study showed that bursts of CG strikes occurred when TCs moved to within 20 km of the shore, and were located in the right front quadrant relative to the storm motion. Lightning flashes were primarily detected in the rainbands for stronger storms, whereas weaker hurricanes generated more lightning flashes within the inner core region. Moreover, she found that in 75% of her data set (12 of 16 TCs), a strong relationship existed between lightning activity within the inner core and the minimum sea-level pressure. *Zhang et al.* [2012] performed a similar study in the northwest Pacific basin. CG lightning activity within 33 landfalling TCs was investigated using the Guangdong Lightning Location System [*Chen et al.*, 2004]. The radial distribution of lightning was found to depend on the intensity of the systems. For tropical storms ($17.2 < v_{max} < 32.6$ m s^{-1}), the ratio of lightning density between the eyewall and the outer rainband was 1:0.5 and it decreased to 1:2.9 for typhoons ($32.7 < v_{max} < 41.4$ m s^{-1}) and 1:8.6 for severe typhoons ($41.5 < v_{max} < 50.9$ m s^{-1}). Eyewall outbreaks were found to occur during four periods: intensity changes (15% of outbreaks for intensification periods and 43% in weakening periods), maximum intensity (15%), and when TCs changed direction (10%).

Fierro et al. [2011] utilized lightning data from the Los Alamos Sferic Array (LASA) [*Shao et al.*, 2005, 2006], a limited-area lightning network that detected both CG and intense intracloud (IC) discharges during the rapid intensification of hurricanes Rita, Katrina, and Charley. They observed an increase in the discharge heights of highly energetic IC flashes that were associated with convective bursts and the strengthening of updrafts.

As their spatial coverage is limited, the NLDN and LASA only permit the study of TCs approaching the coast or making landfall. Other systems, such as the Long-Range Lightning Detection Network (LLDN) or the World Wide Lightning Location Network (WWLLN) allow a detailed analysis of lightning activity (primarily CG lightning strikes) during the entire lifetime of TCs and over large regions (especially the open ocean). *Squires and Businger* [2008] used the LLDN to examine the electrical signature of hurricanes Rita and Katrina (2005). They found that lightning flashes mainly occurred in the eyewall. Moreover, during the periods of intensification and maximum intensity, they observed a general increase in vertical velocities in the eyewall region, which would be consistent with an enhanced collisional charge separation process (noninductive charging) [*Takahashi*, 1978; *Saunders and Peck*, 1998; *Mansell et al.*, 2005]. The rapid intensification period of Rita and Katrina was associated with episodic lightning outbreaks. This feature may be explained by the concentration of rimed ice particles: a sufficient amount of these mixed-phase particles and supercooled water in vigorous updrafts will provide locally favorable conditions for in situ charging to occur [*Black and Hallett*, 1999]. According to *Squires and Businger* [2008], the sudden increase of lightning activity during the rapid intensification period could not be used to predict an intensity change but this information could be used to confirm that the system was still intensifying.

Price et al. [2009] used the WWLLN data to investigate the relationship between lightning activity and TC intensity in 56 TCs from all cyclonic basins. The maximum sustained wind speed and the total flash rate were found to have a strong correlation ($r = 0.82$). They showed that the maximum of lightning activity occurred, on average, 30 h prior to maximum intensity. However, as pointed out by *DeMaria et al.* [2012], these results were obtained by choosing the lag (from 4 days before to 2 days after) that maximized the correlation between maximum sustained wind speed and lightning for each storm. *Abarca et al.* [2011] were the first to study lightning activity in a large set of TCs (24 in total) in the Atlantic basin using the WWLLN. Results from the WWLLN were compared to data from the NLDN when systems came within 400 km of the coasts. They showed that tropical depressions and storms generated more flashes than hurricanes. The radial distribution

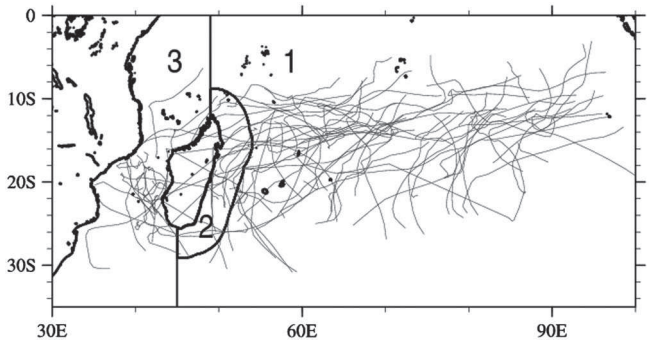

Figure 1. Tracks of the 70 systems from cyclone seasons 2005/2006 to 2012/2013 at intensities of moderate tropical storm, strong tropical storm, tropical cyclone, and intense tropical cyclone. The thick black lines delimit the three subregions considered: 1—open ocean, 2—region near the eastern coast of Madagascar (to 400 km offshore), and 3—Mozambique Channel.

was consistent with the results of *Molinari et al.* [1999]. A relevant finding was also highlighted: lightning density in the inner core of intensifying systems was higher than in that of nonintensifying ones, especially during the weaker storm stages. *DeMaria et al.* [2012] obtained different results in their analysis of 172 TCs from the Atlantic and East/Central Pacific basins using the WWLLN. First of all, they showed that lightning activity within a TC was very sporadic, in agreement with the findings of *Zhang et al.* [2012]. They found that lightning density decreased radially outward with hurricanes generating less lightning overall than weaker systems. Moreover, intensifying storms had a higher lightning density than weakening hurricanes. Based on these results, they concluded that bursts of lightning within the inner core could be useful for forecasting the end of a period of rapid intensification, while heightened lightning activity within the outer rainbands was a surrogate for imminent intensification of the system. They also showed that TCs in the Atlantic basin had higher lightning densities than those in the East/Central Pacific basin.

Total lightning activity (CG + IC) within TCs can also be investigated from satellite observations. *Cecil and Zipser* [1999] studied the relationship between lightning activity and storm intensity using the Optical Transient Detector (OTD) data, while *Cecil et al.* [2002] studied 261 swaths over 45 hurricanes from the Lightning Imager Sensor (LIS). The radial distribution of lightning activity in these studies was consistent with that observed by *Molinari et al.* [1999]. *Cecil and Zipser* [1999] did not find a clear relationship between inner core lightning activity and TC intensification. More recently, the study by *Jiang et al.* [2013], using a large sample of TRMM TC overpasses (over 5000), proposed a bimodal distribution of lightning flashes, with the inner core being the most electrically active region of a TC. This result tends to confirm the distribution observed by *Squires and Businger* [2008]. However, because the OTD and LIS data do not provide continuous coverage of lightning within TCs, they are, by their design, not the most suitable tool for examining the relationship between lightning activity and intensity change. A better monitoring of lightning activity from space will soon be possible with the upcoming launch of GLM (Geostationary Lightning Mapper) [*Goodman et al.*, 2013] on board of the Geostationary Operational Environmental Satellite R-series (GOES-R) and LI (Lightning Imager) [*Grandell et al.*, 2013] on board the Meteosat Third Generation (MTG).

TC activity in the South West Indian Ocean (SWIO) represents 10–12% of the total annual TC activity [*Neumann*, 1993]. This basin spreads from 30°E to 90°E and from the equator to 40°S (Figure 1). Two main areas of cyclogenesis are identified in the SWIO: one over the Mozambique Channel and the other over the open ocean. Due to the particular basin configuration with the presence of Madagascar, TCs are expected to behave differently depending on their position: open ocean behavior and/or interaction with land. This led us to define three different regions in the SWIO to analyze the lightning activity detected by the WWLLN within 70 TCs. The study is organized as follows: the data and analysis methods are given in section 2. Section 3 presents the results for storms evolving over open waters, followed by a comparison with storms interacting with land. The relationships between TC intensity change and lightning activity are presented in section 4, followed by the conclusions in section 5.

2. Data and Methodology

2.1. Lightning Data

Lightning data from January 2005 to May 2013 were extracted from the WWLLN database. The WWLLN (http://www.wwlln.net/) is a global coverage ground-based network that detects impulsive signals of very low frequency radiation (3–30 kHz) called "sferics." The "time of group arrival" is used to determine the location of lightning strikes [*Dowden and Rodger*, 2002]. *Rodger et al.* [2009] and *Abarca et al.* [2010] have

Table 1. Percentage of 6 h Periods Without Lightning Activity Over the Open Ocean for Each Intensity Stage (Moderate Tropical Storm, Strong Tropical Storm, Tropical Cyclone, and Intense Tropical Cyclone) for the Eyewall (EW), Inner Rainbands (IR), and Outer Rainband (OR) Regions

	Moderate Tropical Storm	Strong Tropical Storm	Tropical Cyclone	Intense Tropical Cyclone
EW	66.6	63.7	75.1	61.7
IR	67.9	68.4	75.1	72.8
OR	81.8	81.3	78.5	77.8

evaluated the location accuracy of the WWLLN: the first study showed a global spatial dependence (about 10–20 km in particular for the SWIO) and the second showed that the WWLLN had a northward (4.03 km) and westward (4.98 km) bias for the U.S. region. More recently, *Soula et al.* [2011] observed lightning flashes well colocated with the coldest cloud top temperatures in an isolated storm near Réunion Island (21°S; 55.5°E), in the Indian Ocean. Lightning flash rates detected by the WWLLN were compared to those recorded by a video camera and showed the same trend.

IC and CG lightning flashes are both detected by the WWLLN, but because CG flashes produce the largest peak currents overall, these are the flashes that the network mainly records. *Abarca et al.* [2010] have shown that the CG detection efficiency (DE) is about twofold that of IC flashes. They also tried to quantify the CG DE using data from the NLDN. They showed that the WWLLN's DE improved from 3.88% in 2006 to 10.30% in 2010. When both IC and CG were considered, the WWLLN's DE increased from 2.31% to 6.19% in their subject area (U.S. territory and adjacent waters). *DeMaria et al.* [2012] computed the WWLLN's DE in the Atlantic and East/Central Pacific basins as the ratio between the annual average flash density for each year and the average LIS/OTD flash density over the same domain. For the Atlantic respectively East Pacific) basin, the DEs ranged from 2.6% (respectively 0.9%) in 2005 to 20% (respectively 17.5%) in 2010. *Bovalo et al.* [2012] used the same method but found a smaller increase of the DE in the SWIO basin: from 2.0% in 2005 to 10.9% in 2013.

Even though the WWLLN's DE has increased in recent years, it still remains low. To obtain more "realistic" values, *DeMaria et al.* [2012] scaled up their results using the LIS/OTD annual mean lightning climatology. The WWLLN data were multiplied by the inverse of the DE in each region. In the present work, the WWLLN data were calibrated following this procedure.

The WWLLN's low DE raises some questions regarding the analysis of lightning activity within TCs as they tend to produce a small number of flashes overall. Hence, a period without lightning activity could either arise from unfavorable in-cloud conditions for in situ electrification or from weak lightning activity not readily detected by the low-DE network. Table 1 presents the percentage of 6 h periods without lightning activity over the open ocean. It is noteworthy that lightning activity within a TC is sporadic, as pointed out by *DeMaria et al.* [2012]. Moreover, as the distance from the storm center increases, the proportion of 6 h periods without lightning activity also increases. It becomes obvious that including or excluding periods without lightning will modulate the results. To avoid any ambiguity, the 6 h periods without lightning activity are not considered.

2.2. Best Track

The data were obtained from the Regional Specialized Meteorological Centre (RSMC) La Réunion best track data set. This data set includes the latitude and longitude of the storm center, the 10 min averaged maximum wind speed v_{max} (in kt where 1 kt = 0.514 m s^{-1}), the radius of maximum wind (RMW), and the radius of the outer closed isobar (ROCI) every 6 h. In the SWIO, the RMW is estimated, thanks to microwave images. When an eye is visible on infrared images, the RMW is defined as the mean radius of the −50°C isotherm [*Kossin et al.*, 2007]. Being the only RMW estimation available (no routine penetration flights in this region of the world), RMW estimation errors cannot be explicitly determined. Four categories of TC were defined, based on the classification of the RSMC La Réunion and the presence of an RMW: moderate tropical storm ($34 < v_{max} < 47$ kt, MTS), strong tropical storm ($48 < v_{max} < 63$ kt, STS), tropical cyclone ($64 < v_{max} < 89$ kt, TC), and intense tropical cyclone ($v_{max} > 90$ kt, ITC). In total 70 systems, from MTS to ITC, were investigated, corresponding to 1281 6 h periods. One could note that the storm intensity scale used at the RSMC La Réunion is closely similar to the Saffir-Simpson scale. The radial distributions of lightning activity have also been performed with this scale and will be discussed in section 3.1.

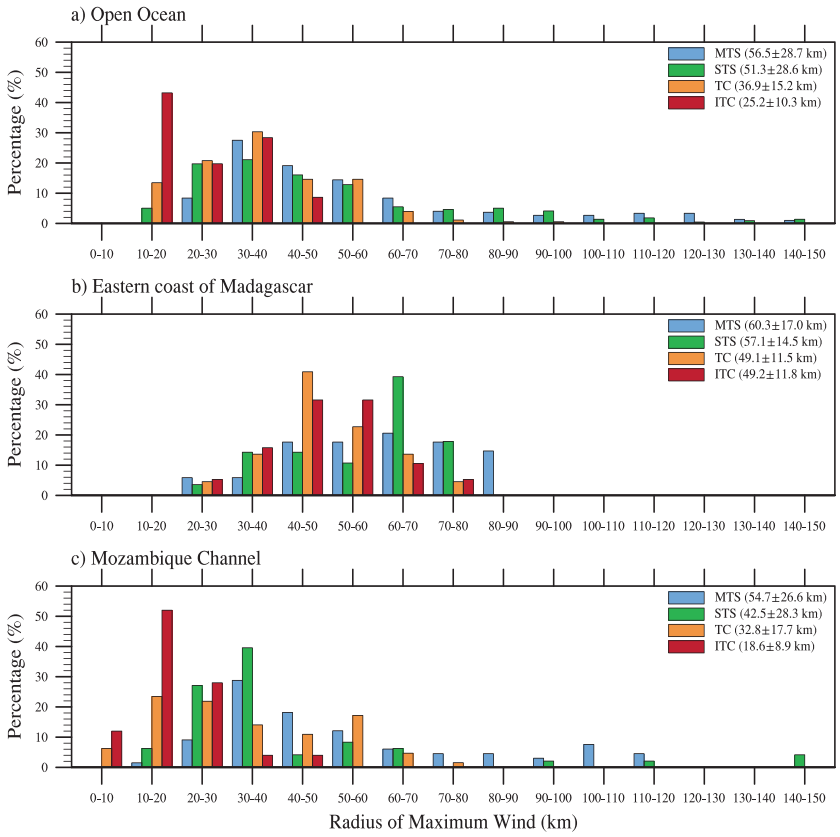

Figure 2. Distribution of the radius of maximum wind (RMW) for systems in the SWIO according to the intensity stage (MTS, STS, TC, and ITC) for systems (a) over the open ocean, (b) within 400 km of the eastern coast of Madagascar, and (c) in the Mozambique Channel. The numbers in parentheses correspond to the mean and standard deviation for each stage and each subdomain.

2.3. Methodology

Figure 1 shows the tracks of the 70 systems analyzed in this work. TCs are mainly located north of 25°S and propagate westward. Due to the configuration of the basin, three regions stand out, where the tropical cyclones and the associated lightning activity are expected to behave differently. Systems can (i) interact with the eastern coast of Madagascar (ECM, region 2 in Figure 1), (ii) develop and/or propagate in the Mozambique Channel (region 3 in Figure 1), or (iii) move over the open ocean (region 1 in Figure 1).

Figure 2 displays the distribution of RMW for TCs in these three regions according to the intensity stage. This figure highlights two characteristics: (i) TCs in the Mozambique Channel (Figure 2c) tend to have smaller RMWs than those in the other regions (Figure 2a) and (ii) TCs near the ECM have the largest RMWs (Figure 2b). These features are more marked for ITC cases: the mean RMWs are 25.2 km over the open ocean, 49.2 km near the ECM, and 18.6 km in the Mozambique Channel. So lightning activity will be studied in each region separately. In this data set, systems interacted with the eastern coast of Madagascar (region 2 in Figure 1) during a total of 145 6 h periods (11.32% of our database). For 18.42% of the 6 h periods (236 6 h periods) systems developed and/or propagated in the Mozambique Channel. The remaining 70.26% of the 6 h periods related to systems over the open ocean.

The radial distribution of lightning activity has already been studied in various ways. *Molinari et al.* [1999] subdivided hurricanes into 20 km annular rings up to 300 km from the storm center. *Abarca et al.* [2010] used the same radial intervals and defined the inner core and the outer rainbands as the regions between 0 and 100 km and between 100 and 300 km, respectively. *Squires and Businger* [2008] studied the distribution of lightning activity within 300 km of the storm center, using 25 km annular rings. They distinguished between the eyewall (0–50 km from the storm center), the inner rainbands (75–175 km from the storm center), and the outer rainbands (region beyond 175 km from the storm center). *DeMaria et al.* [2012] used six radial

intervals: 0–50, 50–100, 100–200, 200–300, 300–400, and 400–500 km. They grouped some regions to form the eyewall (0–50 km), the inner core (0–100 km), and the rainbands (200–300 km).

Jiang and Ramirez [2013] pointed out that the arbitrary radial intervals used in the previous studies may not be optimal. In order to better represent the different regions of each TC, two parameters of the RSMC La Réunion best tracks were used: the RMW to delimit the eyewall and the ROCI for the TC size [*Merill*, 1984; *Kimball and Mulekar*, 2004; *Chan and Chan*, 2012; *Drake*, 2012]. Akin to the RMW, the ROCI also shows dependence on storm intensity and ranges from 406 km for MTS to 484 km for ITC. As shown in the studies mentioned above, lightning activity is mainly located in the eyewall and the rainbands. Based on this radial distribution and preliminary results, only three regions were used to define a TC, similar to *Jiang* [2012]. In the present work, the eyewall is defined as the region between the storm center and 1.5 × RMW to consider eyewall tilting. The inner rainbands are located between 1.5 × RMW and 3 × RMW. Finally, the outer rainband region is the region between 3 × RMW and ROCI.

The storm motion vector was estimated from the angle between two successive positions. Then, the position of each lightning strike was computed relative to the motion vector (0° being the motion direction).

The intensity change was obtained using the difference in v_{max} (called Δv_{max}) between two consecutive 6 h periods: if this difference is positive (respectively negative), the system is intensifying (respectively weakening). Four different thresholds were defined: $0 < \Delta v_{max} < 6.6$ kt $(6\text{ h})^{-1}$ (slow intensification), $\Delta v_{max} \geq 6.6$ kt $(6\text{ h})^{-1}$ (rapid intensification), $0 > \Delta v_{max} > -6.6$ kt $(6\text{ h})^{-1}$ (slow weakening), and $\Delta v_{max} \leq -6.6$ kt $(6\text{ h})^{-1}$ (rapid weakening). These thresholds were based on the definition of the rapid intensification ($\Delta v_{max} \geq 30$ kt in 24 h) proposed by *Kaplan and DeMaria* [2003] and *Kaplan et al.* [2010] but extended to the weakening phase. In the Atlantic basin, maximum winds refer to 1 min sustained winds while, in the SWIO, 10 min averaged winds were used to define the maximum wind. Thus, a conversion factor of 0.88 was applied to obtain a rapid intensification definition for this basin [*Caroff et al.*, 2010].

3. Radial and Azimuthal Distributions

Results presented in this section have been statistically tested, and each sample is normally distributed at the 99% level.

3.1. Radial Distribution

Figure 3a displays the geometric mean of the radial distribution of lightning activity for TCs over open ocean and stratified by intensity: MTS, STS, TC, and ITC stages. Due to the high variability of the lightning density [see *DeMaria et al.*, 2012, Figure 2], the geometric mean was chosen because it is less sensitive to extreme values than the arithmetic mean. As the distance from the storm center increases, lightning activity decreases; flashes are mainly detected in the eyewall region regardless of storm intensity. Lightning activity in the eyewall is less intense at the STS stage (28 flashes km^{-2} yr^{-1}) and increases with storm intensity (54 flashes km^{-2} yr^{-1} for the TC stage and 52 flashes km^{-2} yr^{-1} for the ITC stage). Lightning activity within the inner rainbands is quite similar for MTS, STS, and TC stages (~20 flashes km^{-2} yr^{-1}) while for the ITC stage, it reaches 48 flashes km^{-2} yr^{-1}. Lightning activity in the outer rainbands is relatively small, not exceeding 8 flashes km^{-2} yr^{-1} regardless of storm intensity.

The radial distribution of lightning activity over the open ocean is broadly consistent with the studies of *DeMaria et al.* [2012] and *Jiang et al.* [2013] with the bulk of the lightning primarily located in the eyewall. The most noticeable difference is found in the inner rainbands, where the two previous studies found small lightning activity. The different instruments and methodologies used in each study might be responsible for these differences: WWLLN (land based, global coverage, and low DE) and fixed radius for all systems for *DeMaria et al.* [2012] and TRMM mission (satellite, low Earth orbit, and high DE) and subjective analysis for *Jiang et al.* [2013].

The main distribution obtained in Figure 3a can be explained by the distribution of hydrometeors in the eyewall [*Houze*, 2010; *Black et al.*, 1996] and the distribution of updrafts/downdrafts in the eyewall and principal rainband [*Houze*, 2010; *Fierro et al.*, 2007; *Didlake and Houze*, 2009; *Fierro and Reisner*, 2011; *Didlake and Houze*, 2013]. For the modeling works, even if lightning activity was overestimated, the principal region of lightning discharge triggering was the eyewall [*Fierro et al.*, 2007; *Fierro and Reisner*, 2011]. One of the hypotheses explaining the propagation mechanism of rainbands is that they act like a squall line. However, observational studies [*Petersen et al.*, 1999; *Orville et al.*, 1997] have shown that this convective system has

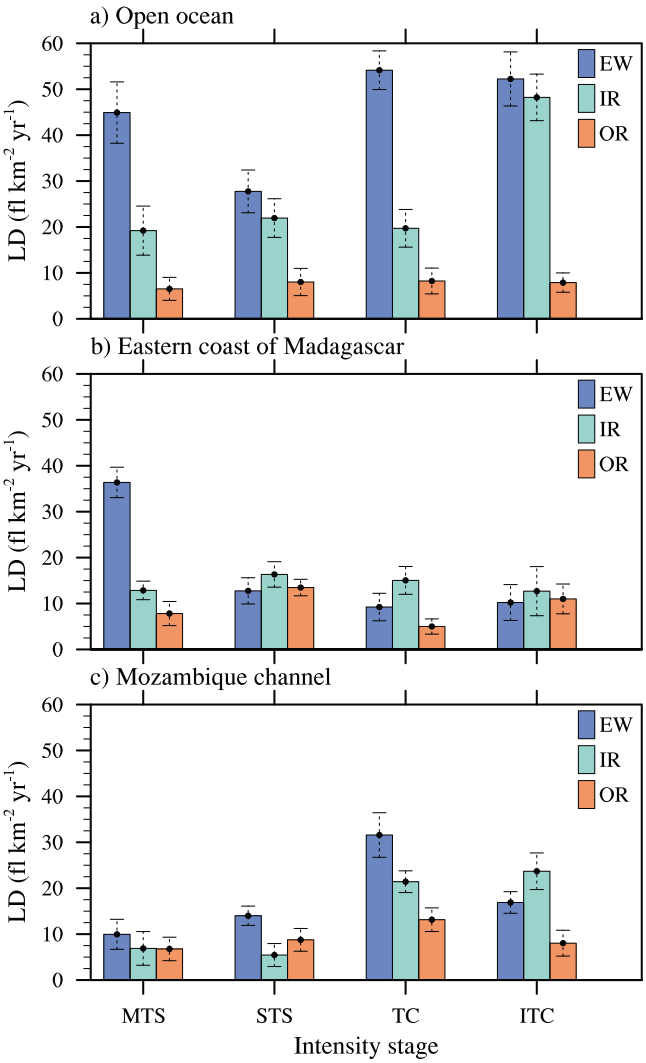

Figure 3. Radial distribution of lightning density (flashes km^{-2} yr^{-1}) according to the intensity stage (MTS, STS, TC, and ITC) for (a) the open ocean, (b) the eastern coast of Madagascar, and (c) the Mozambique Channel. The blue, green, and orange bars correspond to the eyewall (EW), the inner rainbands (IR), and the outer rainband (OR), respectively. The error bars represent the standard deviation.

little lightning activity. Even if the convective cells are electrified, the electric field is not enough intense to initiate an electrical discharge. *Fierro et al.* [2007] also obtained poor hydrometeor content and limited electric field in an idealized tropical cyclone.

The geometric mean of the radial distribution of lightning activity in the ECM is shown in Figure 3b. When systems are within 400 km of the eastern coast of Madagascar, lightning activity in MTSs is maximum in the eyewall region, and then decreases with the distance from the storm center. For STS, TC, and ITC, lightning density is maximum in the inner rainbands (~14–17 flashes km^{-2} yr^{-1}). Furthermore, lightning density in the eyewall of systems close to Madagascar is much less intense than for systems over the open ocean.

It was expected that lightning activity increases when approaching land. Indeed, several studies have shown the beneficial effect of land on convection: increase of friction [*Tuleya and Kurihara*, 1978], favorable environmental conditions [*Bogner et al.*, 2000; *Baker et al.*, 2009; *Eastin and Link*, 2009; *Houze*, 2010], or increase of continental aerosol particles [*Khain et al.*, 2008b]. However, these particles or CCN (for Cloud Condensation Nuclei) enhance convection in the rainbands and reduce it in the eyewall. The smaller lightning activity in the core (eyewall + inner core) of systems near the ECM may be due to intrusions of CCN into storm center. Moreover, these results differ from *Molinari et al.* [1999] and *Abarca et al.* [2011]. Regional atmospheric conditions and different type of continental CCN in the SWIO may explain these differences.

In the Mozambique Channel (Figure 3c), the radial distribution of lightning flashes is different at each intensity stage. As in the other two regions, during the MTS stage, lightning activity is more intense in the eyewall than in the rainbands. However, in contrast to systems evolving over the open ocean and the ECM, lightning activity is rather low (> 10 flashes km^{-2} yr^{-1} in each region). For systems at the STS stage, the lightning density shows a maximum in the eyewall and a gap in the inner rainbands. The distribution of lightning flashes within TCs is similar than the geometric mean of all systems over open ocean. During the ITC stages, however, the lightning density is higher in the inner rainbands.

TCs in the Mozambique Channel are surrounded by land, which can explain the great variability with respect to intensity and the difference in lightning behavior with the ECM. As seen in Figure 1, systems moving through the Mozambique Channel can exhibit different kinds of track and can make landfall over the eastern coast of Africa or over the western coast of Madagascar. The complexity of the trajectories in this region makes the analysis of lightning activity more difficult than in the other regions. Moreover, the size of TCs can

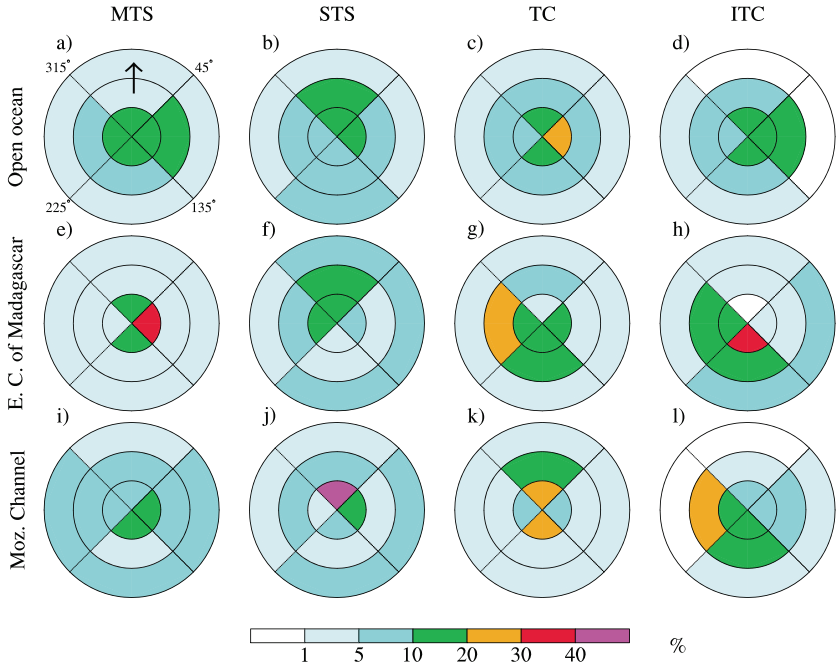

Figure 4. Horizontal distribution of lightning density (%) relative to storm motion. (a–d) The open ocean. (e–h) The ECM. (i–l) The Mozambique Channel. The front, right, rear, and left quadrants are respectively the regions 315°–45°, 45°–135°, 135°–225°, and 225°–315°. The concentric circles correspond to the eyewall (EW), the inner rainbands (IR), and the outer rainbands (OR). The arrow represents the storm motion.

influence the behavior of lightning activity as, for example, "midgets" would have a more oceanic pattern. The understanding of lightning activity distribution in this region requires better knowledge of the trajectory and TC size. As pointed out by *Abarca et al.* [2011], when considering interactions with land, the angle between the storm motion and the coast is also important.

Results obtained when using the Saffir-Simpson scale (not shown) are globally similar to the preceding radial distributions. Lightning activity over open ocean is mainly found in the eyewall and in the inner core; the only difference is that more lightning flashes are found in the eyewall during the ITC stage. Near the ECM, the maximum of lightning activity occurs for the STS stage instead of the MTS stage. In the Mozambique Channel, lightning activity during TC stages is slightly reduced. The findings presented here are thus consistent with previous studies focusing in other cyclonic regions.

3.2. Azimuthal Distribution Relative to Storm Motion

Figure 4 illustrates the azimuthal distribution of lightning activity relative to storm motion in the three regions, which allows relevant lightning asymmetries to be identified and quantified.

Over the open ocean (Figures 4a–4d), as shown in Figure 3a, lightning activity is concentrated in the eyewall and decreases outward. In the outer rainband, lightning activity is low (<10%) regardless of storm intensity. During MTS stages, lightning flashes are produced uniformly in the eyewall (10–20% per quadrant) while, in the inner rainbands, lightning activity is mainly located in the right quadrant (10–20%). At STS intensity, most lightning occurs in the front and the right quadrants in the eyewall (10–20%) and the front quadrant in the inner rainbands (10–20%). When the storm intensifies to TC, lightning activity within the eyewall becomes concentrated in the right quadrant as 20 to 30% of the overall lightning flashes occur in this region. During ITC intensity, lightning activity is quite uniform in the eyewall and has a maximum in the right quadrant of the inner rainbands.

In the ECM (Figures 4e–4h), at MTS intensity, lightning flashes in the eyewall are primarily found in the right quadrant (30–40%) while lightning activity in the inner and outer rainband regions is quite uniform (<5%). For the STS stage, the eyewall front and left quadrants are the regions where lightning flashes are preferentially detected (10–20%). In the inner rainbands, this trend is also present but lightning activity dominates in the front quadrant. At TC and ITC intensities, lightning flashes are mainly produced in the left and rear

quadrants of the storm. During the TC stage, lightning activity is located in the left side of the inner rainbands (20–30%) while, during the ITC, it is found in the rear quadrant of the eyewall (30–40%).

For systems at the MTS stage in the Mozambique Channel (Figure 4i), lightning activity dominates in the rear and right quadrants in the eyewall (10–20%). At the STS stage (Figure 4j), lightning flashes are mainly detected in the front quadrant of the eyewall (> 40%). At TC intensity, the front and rear quadrants concentrate more than 40% of all lightning activity. During the ITC stage, the left quadrant of the inner rainbands is the preferred region for lightning (20–30%). In the eyewall and inner rainbands, the left and rear quadrants show more than 50% of the whole lightning activity at ITC intensity.

Abarca et al. [2011] studied the azimuthal distribution of lightning flashes relative to storm motion in 24 tropical cyclones over the open ocean in the Atlantic basin. They stratified their data set according to storm motion (slow, moderate, and fast motion). They showed that for slowly moving storms, lightning activity in the eyewall was largely found in the front quadrants or in the right rear quadrant. For moderately to fast moving storms, lightning flashes were generated in the right quadrants, with a preference for the right rear quadrant. In the present study, the data set was not stratified according to the speed of travel. The basin configuration and the intensity stage are important factors in explaining the azimuthal distribution of lightning activity in the ECM and in the Mozambique Channel. In particular, the location of lightning flashes can be influenced by parameters such as the storm motion, the TC speed, the angle between the storm center and the shore, or the wind shear.

4. Relationships Between Intensity Change and Lightning Activity Over the Open Ocean

In this section, some categories have been grouped to increase the sample size and to facilitate the interpretation of the results. Only two intensity categories are considered: TS (MTS + STS) and TC (TC + ITC). Moreover, only lightning activity over the open ocean is examined, and results are presented from a qualitative point of view. As in *Abarca et al.* [2011], an individual time period (ITP) refers to a 6 h period between two consecutive Best Track times. To focus on the lightning activity frequency, the percentage of ITPs with lightning activity was computed.

Figures 5 and 6 represent the percentage of ITPs with lightning activity during each intensity change: slow or rapid intensification/weakening. When TSs intensify (Figures 5a–5c), there is no obvious signal in the eyewall or the inner rainband regions for either slow or rapid intensifications. In these regions, ~40% of the ITPs have lightning activity. In the outer rainbands, the percentage of ITPs with lightning activity is greater by a factor 4 between −18 h and 0 h, ranging from 5% to 20% when TSs intensify rapidly.

When the systems reach the TC intensity (Figures 5d–5f), there is a significant difference between rapidly and slowly intensifying systems. Lightning activity is more likely to occur during periods of rapid intensification. For rapidly intensifying TCs, as for TSs, ~40% of the ITPs exhibit lightning activity in the eyewall. The same behavior is observed in the inner and outer rainband regions: the percentage of electrically active ITPs is significantly larger for TCs that intensify rapidly than for TCs with low intensification rates. For the latter, the percentage of ITPs with lightning activity in the eyewall (respectively inner rainbands) is smaller by a factor 3, falling from 30% (respectively 24%) at −24 h to 10% (respectively 8%) at the time of the intensity change.

During the weakening phases (Figure 6), the differences in lightning activity are more pronounced between storms experiencing low and high weakening rates. Lightning activity is more frequent during rapid weakening than during slow weakening in the three regions.

Concerning the rapid weakening of TS cases, the proportion of ITPs with lightning activity in the eyewall decreases between −24 h and −6 h (50% to 45%) and from −6 h the slope of the curve is steeper. A similar feature is observed in the inner rainband region, but the change in the slope is less marked and occurs at the time of the rapid weakening. In the outer rainbands, the percentage of ITPs with lightning activity increases from 35% at −18 h to 50% at −6 h and decreases afterward.

As for TCs undergoing rapid intensification, TCs that weaken rapidly have a greater proportion of ITPs with lightning activity (nearly 3 times more) than those that weaken slowly. Even if this difference is considerable,

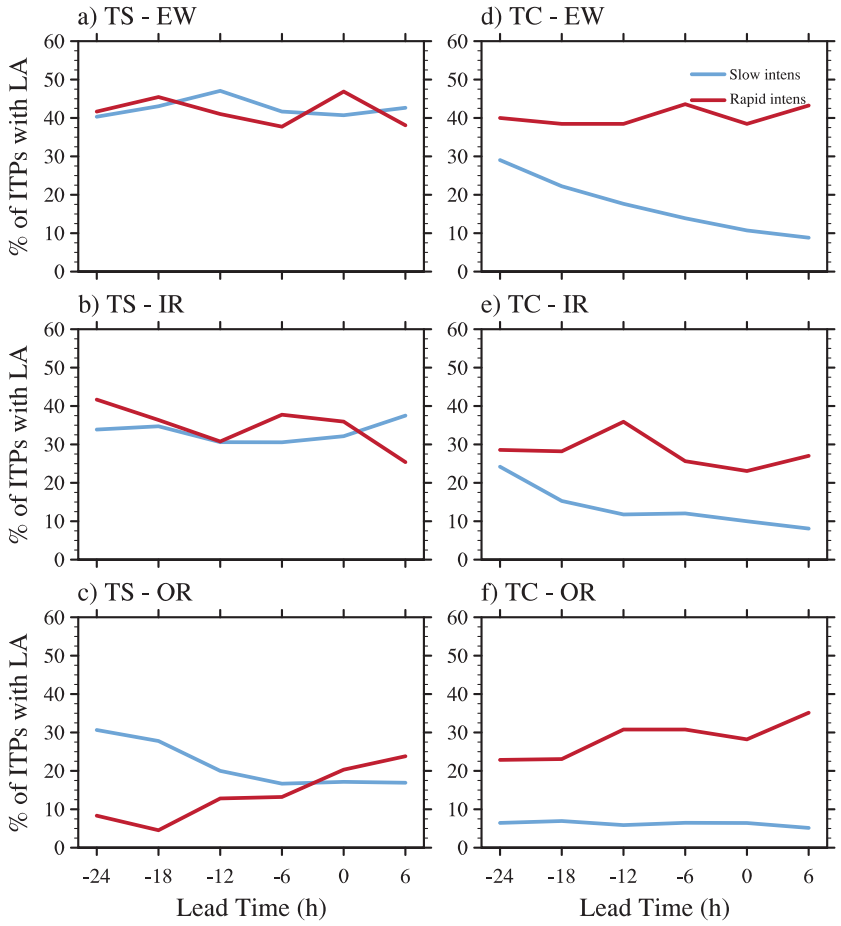

Figure 5. Percentage of ITPs with lightning activity relative to the lead time from intensification (−24h,…0,…,+6h) for (a–c) TS cases and (d–f) TC cases over the open ocean. Figures 5a and 5d correspond to the eyewall region (EW), Figures 5b and 5e to the inner rainbands region (IR), and Figures 5c and 5f to the outer rainband region (OR). Two thresholds are used for the rate of intensification: $0 < \Delta v_{max} < 6.6$ kt $(6\ h)^{-1}$ (blue curves) and $\Delta v_{max} \geq 6.6$ kt $(6\ h)^{-1}$ (red curves).

the percentage of ITPs with lightning activity near or during weakening periods does not seem to be useful for forecasting rapid weakening.

The main results reported here bear some similarities with those proposed by *DeMaria et al.* [2012] and *Jiang and Ramirez* [2013]. Although these studies focused on the lightning density rather than the frequency of lightning activity, they showed that a negative relationship existed between lightning activity and storm intensification. The results displayed in Figures 5d and 5e are similar: this decrease of lightning activity occurs at TC intensity and for slow intensifications. In the outer rainbands of rapidly intensifying TSs, the proportion of ITPs with lightning activity increases as the storms deepen. The outer rainbands are far from the inner core and thus are unconstrained by the dynamics of the inner core [*Houze*, 2010]. This increase in the frequency of lightning activity in the outer rainbands is thus consistent with the results from *Jiang and Ramirez* [2013]: during rapid intensification, convection in the outer rainbands is enhanced due to the favorable environmental conditions rather than to internal processes. Moreover, as in *DeMaria et al.* [2012], a strong signal in lightning activity in the eyewall is also visible during periods of rapid weakening of TSs.

According to *DeMaria et al.* [2012], lightning activity in the inner core during a period of rapid intensification should be linked to the environment, particularly to vertical shear. The storm can intensify due to an interaction between the environmental shear and the inner core potential vorticity. The vertical shear may tilt the vortex, resulting in intense asymmetric convection in the eyewall/inner core. These convective bursts are favorable to the production of lightning activity. However, the vertical wind shear can also suppress the existing convection and put an end to the short-term intensification. Other studies also show that short-lived convective bursts participate in the rapid intensification process. *Kelley et al.* [2004] suggest that

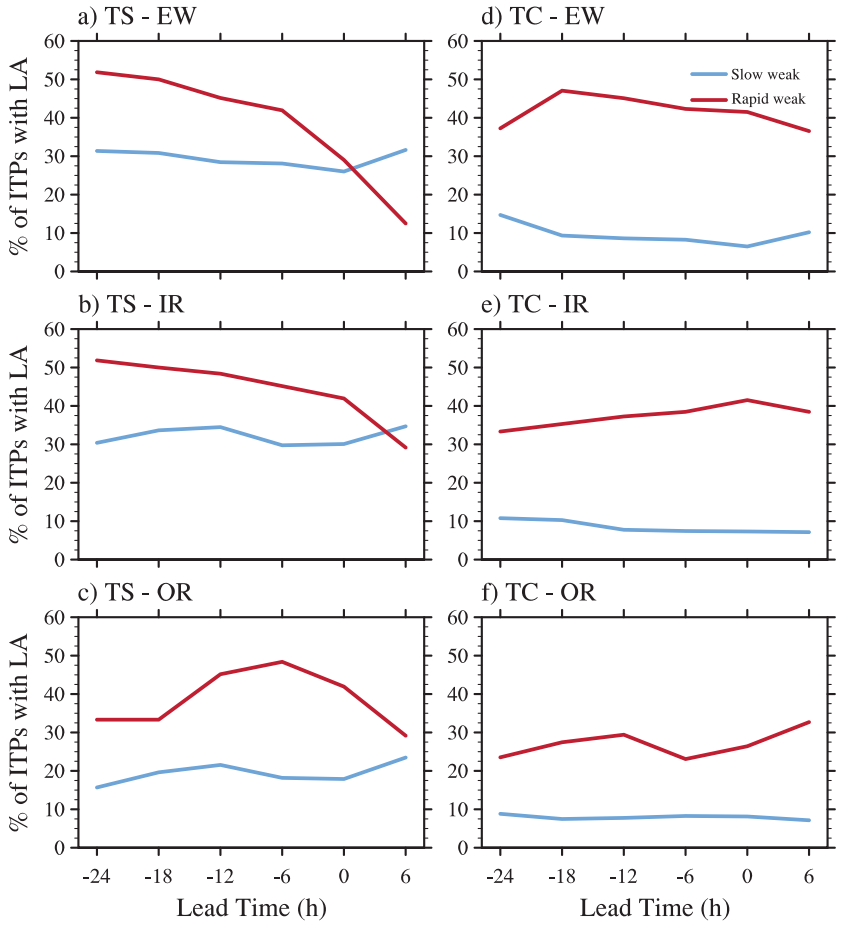

Figure 6. Same as Figure 5 but for weakening cases. Two thresholds are used for the rate of weakening: $0 > \Delta v_{max} > -6.6$ kt (6 h)$^{-1}$ (blue curves) and $\Delta v_{max} \leq -6.6$ kt (6 h)$^{-1}$ (red curves).

the presence of such events in the eyewall may be a signal of ongoing intensification. *Rogers* [2010] simulated hurricane Dennis (2005, Atlantic basin) and observed convective bursts inside the radius of maximum wind 6 h prior to rapid intensification. They concluded that there was a "synergistic relationship between convective bursts and the background secondary circulation" before rapid intensification. Rapid intensification could also arise from an increase in updraft mass flux. Based on the Tropical Rainfall Measuring Mission (TRMM) data, *Kelley and Halverson* [2011] found that in strong (respectively weak) tropical cyclones, convective bursts in the eyewall, persisting for at least 12 h, could cause an intensification of 16 (respectively 9) m s^{-1}. They argue that convective bursts permit extra latent heat to be released from the boundary layer in the free troposphere. The tropical cyclone vortex converts this latent heat into kinetic energy of the primary circulation through "a special case of the general geostrophic adjustment problem" [*Nolan et al.*, 2007]. However, *Kelley and Halverson* [2011] preferred the latent heat (only latent heat of condensation and evaporation) instead of enthalpy in order to use the energy efficiency calculated by *Nolan et al.* [2007].

Fierro et al. [2011] and *Fierro and Reisner* [2011] analyzed the lightning activity within hurricane Rita (2005) using observations and a simplified electrical scheme, respectively. The results showed that lightning bursts within the eyewall were associated with convective events (CE) during the period of rapid intensification. During the reintensification of the remnant Tropical Storm Erin (2007; Atantic basin), lightning activity (mainly IC flashes) was detected by the Oklahoma Lightning Mapping Array (LMA) [*Rison et al.*, 1999; *Thomas et al.*, 2004] and was well correlated to the maximum sustained wind speed. During its reintensification period, the maximum of lightning activity was found in an eyewall CE with deep convective updrafts, consistent with *Kelley et al.* [2004] and *Fierro et al.* [2011].

These results may explain why lightning activity within hurricanes is generally sporadic.

5. Conclusions

Lightning data from the WWLLN have been used to study lightning activity within TCs of the SWIO for cyclone seasons 2005/2006 to 2012/2013. The radial and azimuthal distributions according to intensity stages (MTS, STS, TC, or ITC) have been investigated. Based on the basin configuration, lightning activity within tropical cyclones has been studied for three different regions: over the open ocean, near the ECM (to a distance of 400 km offshore), and in the Mozambique Channel. The relationship between lightning activity and intensity change has also been studied but only over the open ocean.

The radial distribution of lightning activity is affected by the location and the storm intensity. Lightning activity depends on the intensity stage, but in contrast to previous findings, lightning density in the eyewall is greater at higher intensity (TC and ITC) over the open ocean. Moreover, lightning activity is primarily found in the eyewall, regardless of storm intensity in this region. Lightning in all regions is similar over the ECM while, in the Mozambique Channel, the eyewall is the main region where lightning activity is detected.

The azimuthal distribution showed that the front and right quadrants are the preferred regions for lightning production over the open ocean. In the other two regions, the distribution is more complex because of the interaction with land. However, in all regions, no obvious connection was observed between lightning distribution and cyclone intensity but the studies by *Corbosiero and Molinari* [2003] and *Abarca et al.* [2011] suggest that vertical wind shear is also among the key components explaining the distribution of lightning activity.

The relationship between lightning activity and intensity change has been studied using different thresholds of intensification and weakening but only over the open ocean. Intensity is stratified into two main categories to facilitate the interpretation of the results. For TS cases, in the outer rainbands, an increase in the proportion of ITPs with lightning activity is observed as the storm intensifies. At TC intensity, regardless of the region, there are more periods with lightning activity prior to a rapid intensification. For low intensification rates, the frequency of lightning activity decreases in the eyewall and in the inner rainbands. When TSs weaken rapidly, the proportion of ITPs with lightning activity in the eyewall and in the inner rainbands decreases. The converse is observed in the outer rainbands.

Although this work is the first presenting an analysis of the lightning behavior and distribution within TCs in this relatively remote region of the world, the analysis procedures employed here suffer from noteworthy limitations. Although the RMW is more representative of a key structural aspect of mature TCs, the definition of the inner rainband (1.5–3 × RMW) may not be applicable to all systems and for all intensities. A new method to determine the TC size has recently been proposed by *Knaff et al.* [2014] and will be tested in a future work. Moreover, the radial distribution of lightning activity displayed here is the one detected by the WWLLN. Recently, *Fierro et al.* [2011] and *Griffin et al.* [2014] have shown that lightning activity in TCs is not as sporadic when using regional high-DE networks that detect both IC and CG flashes (LASA and LMA).

New insights into lightning activity within tropical cyclones will also be possible with the deployment of future satellites. The lightning optical instruments GLM and LI will be on board the next generation GOES-R series and MTG satellites, respectively. The Atlantic basin and a fraction of the SWIO will be covered by these satellites. The monitoring of lightning activity in these regions will be continuous with a high DE of total lightning activity (CG + IC).

Insufficient observations are available for the SWIO, so it is difficult to determine the physical processes involved in tropical cyclone electrification. A better understanding of what might be occurring in tropical cyclones in terms of microphysics and lightning is now possible thanks to explicit electrification studies [*Fierro et al.*, 2007; *Fierro and Reisner*, 2011]. The radial and azimuthal distributions and the potential of lightning activity to forecast intensity change will be examined in ongoing simulations of electrified tropical cyclones in the SWIO.

Acknowledgments
The authors would like to thank the three anonymous reviewers for providing helpful suggestions which improved the quality of the manuscript. Comments of Reviewers 1 and 2 on an earlier version of this study were also very useful. We also thank the World Wide Lightning Location Network, a collaboration among 40 universities and institutions, for providing the lightning locations used in this study. As the University of Réunion Island is a part of this network, the data set used in this study was provided free of charge. Data concerning tropical cyclones are available on the Web site of RSMC La Réunion. Funding for this work was provided by the Fondation MAIF through the PRECYP project. This study is part of C. Bovalo's PhD which was financially supported by La Région Réunion and the European Union Council.

References

Abarca, S. F., K. L. Corbosiero, and T. J. Galarneau Jr. (2010), An evaluation of the World Wide Lightning Location Network (WWLLN) using the National Lightning Detection Network (NLDN) as ground truth, *J. Geophys. Res.*, *115*, D18206, doi:10.1029/2009JD013411.

Abarca, S. F., K. L. Corbosiero, and D. Vollaro (2011), The World Wide Lightning Location Network and convective activity in tropical cyclones, *Mon. Weather Rev.*, *139*, 175–191.

Baker, A. K., M. D. Parker, and M. D. Eastin (2009), Environmental ingredients for supercells and tornadoes within hurricane Ivan, *Weather Forecasting*, *24*, 223–244.

Black, M. L., R. W. Burpee, and F. D. Marks Jr. (1996), Vertical motions characteristics of tropical cyclones determined with airborne Doppler radial velocities, *J. Atmos. Sci.*, *53*, 1887–1909.
Black, R. A., and J. Hallett (1999), Electrification of the hurricanes, *J. Atmos. Sci.*, *56*, 2004–2028.
Bogner, P. B., G. M. Barnes, and J. L. Franklin (2000), Conditional instability and shear for six hurricanes over the Atlantic Ocean, *Weather Forecasting*, *15*, 192–207.
Bovalo, C., C. Barthe, and N. Bègue (2012), A lightning climatology of the South West Indian Ocean, *Nat. Hazards Earth Syst. Sci.*, *12*, 2659–2670, doi:10.5194/nhess-12-2659-2012.
Caroff, P., C. Bientz, T. Dupont, S. Langlade, H. Quetelard, and G. Rayot (2010), *Cyclone Season of South-West Indian Ocean 2009–2010*, Météo France–Direction Interrégionale de La Réunion, Sainte-Clotilde, La Réunion, France.
Cecil, D. J., and E. J. Zipser (1999), Relationships between tropical cyclone intensity and satellite-based indicators of inner core convection: 85-GHz ice-scattering signature and lightning, *Mon. Weather Rev.*, *127*, 103–123.
Cecil, D. J., E. J. Zipser, and S. W. Nesbitt (2002), Reflectivity, ice scattering, and lightning characteristics of hurricane eyewalls and rainbands. Part I: Quantitative description, *Mon. Weather Rev.*, *130*, 769–784.
Chan, K. T. F., and J. C. L. Chan (2012), Size and strength of tropical cyclones as inferred from QuickSCAT data, *Mon. Weather Rev.*, *140*, 811–824.
Chen, S. M., Y. Du, and L. M. Fan (2004), Lightning data observed with lightning location system in Guang-dong province, China, *IEEE Trans. Power Delivery*, *19*(3), 1148–1153.
Corbosiero, K. L., and J. Molinari (2003), The relationship between storm motion, vertical wind shear, and convective asymmetries in tropical cyclones, *J. Atmos. Sci.*, *60*, 366–376.
DeMaria, M., R. T. DeMaria, J. A. Knaff, and D. Molenar (2012), Tropical cyclone lightning and rapid intensity change, *Mon. Weather Rev.*, *140*, 1828–1842, doi:10.1175/MWR-D-11-00236.1.
Didlake, A. C., and R. A. Houze (2009), Convective-scale downdrafts in the principal rainband of hurricane Katrina (2005), *Mon. Weather Rev.*, *137*, 3269–3293.
Didlake, A. C., and R. A. Houze (2013), Convective-scale variations in the inner-core rainbands of a tropical cyclone, *J. Atmos. Sci.*, *70*, 504–523.
Dowden, R. L., and C. J. Rodger (2002), VLF lightning location by time of group arrival (TOGA), *J. Atmos. Sol. Terr. Phys.*, *64*, 817–830.
Drake, L. (2012), Scientific prerequisites to comprehension of the tropical cyclones forecast: Intensity, track and size, *Weather Forecasting*, *27*, 462–472.
Eastin, M. D., and M. C. Link (2009), Miniature supercells in an offshore outer rainband of hurricane Ivan (2004), *Mon. Weather Rev.*, *137*, 2081–2104.
Fierro, A. O., and J. M. Reisner (2011), High-resolution simulation of the electrification and lightning of hurricane Rita during the period of rapid intensification, *J. Atmos. Sci.*, *68*, 477–494.
Fierro, A. O., L. Leslie, E. Mansell, J. Straka, D. MacGorman, and C. Ziegler (2007), A high-resolution simulation of microphysics and electrification in an idealized hurricane-like vortex, *Meteorol. Atmos. Phys.*, *98*, 13–33.
Fierro, A. O., X.-M. Shao, T. Hamlin, J. M. Reisner, and J. Harlin (2011), Evolution of eyewall convective events as indicated by intra-cloud and cloud-to-ground lightning activity during the rapid intensification of hurricanes Rita and Katrina, *Mon. Weather Rev.*, *139*, 1492–1504.
Goodman, S. J., et al. (2013), The GOES-R Geostationary Lightning Mapper (GLM), *Atmos. Res.*, *124–125*, 34–49.
Grandell, J., M. Dobber, and R. Stuhlmann (2013), Geostationnary lightning: Observations in support of NWC and severe weather monitoring, paper presented at European Severe Storms Conference, ESSL, Helsinki, Finland, 3–7 June.
Griffin, E. T., D. MacGorman, M. Kumjian, and A. Fierro (2014), An electrical and polarimetric analysis of the overland reintensification of Tropical Storm Erin (2007), *Mon. Weather Rev.*, *142*, 2321–2344, doi:10.1175/MWR-D-13-00360.1.
Houze, R. A. (2010), Clouds in tropical cyclones, *Mon. Weather Rev.*, *138*, 293–344.
Jiang, H. (2012), The relationship between tropical cyclone intensity change and the strength of inner-core convection, *Mon. Weather Rev.*, *140*, 1164–1176.
Jiang, H., and E. M. Ramirez (2013), Necessary conditions for tropical cyclone rapid intensification as derived from 11 years of TRMM data, *J. Clim.*, *26*, 6459–6470.
Jiang, H., E. M. Ramirez, and D. J. Cecil (2013), Convective and rainfall properties of tropical cyclone inner core and rainbands from 11 years of TRMM data, *Mon. Weather Rev.*, *141*, 431–450.
Kaplan, J., and M. DeMaria (2003), Large-scale characteristics of rapidly intensifying tropical cyclones in the North Atlantic basin, *Weather Forecasting*, *18*, 1093–1108.
Kaplan, J., M. DeMaria, and J. A. Knaff (2010), A revised tropical cyclone rapid intensification index for the Atlantic and Eastern North Pacific basins, *Weather Forecasting*, *25*, 220–241.
Kelley, O. A., and J. B. Halverson (2011), How much tropical cyclone intensification can result from the energy released inside of a convective burst?, *J. Geophys. Res.*, *116*, D20118, doi:10.1029/2011JD015954.
Kelley, O. A., J. Stout, and J. B. Halverson (2004), Tall precipitation cells in tropical cyclone eyewalls are associated with tropical cyclone intensification, *Geophys. Res. Lett.*, *31*, L24112, doi:10.1029/2004GL021616.
Khain, A., N. Cohen, B. Lynn, and A. Pokrovsky (2008b), Possible aerosol effects on lightning activity and structure of hurricanes, *J. Atmos. Sci.*, *65*, 3652–3677.
Kimball, S. K., and M. S. Mulekar (2004), A 15-year climatology of North Atlantic tropical cyclones. Part I: Size parameters, *J. Clim.*, *17*, 3555–3575.
Knaff, J. A., S. P. Longmore, and D. A. Molenar (2014), An objective satellite-based tropical cyclone size climatology, *J. Clim.*, *27*, 455–476.
Kossin, J. P., J. A. Knaff, H. I. Berger, D. C. Herndon, T. A. Cram, C. S. Velden, R. J. Murnane, and J. D. Hawkins (2007), Estimating hurricane wind structure in the absence of aircraft reconnaissance, *Weather Forecasting*, *22*, 89–101.
Lyons, W. A., and C. S. Keen (1994), Observations of lightning in convective supercells within tropical storms and hurricanes, *Mon. Weather Rev.*, *122*, 1897–1916.
Mansell, E. R., D. R. MacGorman, C. L. Ziegler, and J. M. Straka (2005), Charge structure and lightning sensitivity in a simulated multicell thunderstorm, *J. Geophys. Res.*, *110*, D12101, doi:10.1029/2004JD005287.
Merill, R. T. (1984), A comparison of large and small tropical cyclones, *Mon. Weather Rev.*, *112*, 1408–1418.
Molinari, J., P. Moore, and V. Idone (1999), Convective structure of hurricanes as revealed by lightning locations, *Mon. Weather Rev.*, *127*, 520–534.
Nagele, D. (2010), Analysis of cloud-to-ground lightning within tropical cyclones, MS thesis, 89 pp., Texas Tech Univ., Lubbock.

Neumann, C. (1993), Global overview, in *Global Guide to Tropical Cyclone Forecasting*, edited by G. J. Holland, 43 pp., WMO Trop. Cyclone Program Rep. TCP-31, World Meteorol. Organ., Geneva, Switzerland.

Nolan, D. S., Y. Moon, and D. P. Stern (2007), Tropical cyclone intensification from asymmetric convection: Energetics and efficiency, *J. Atmos. Sci.*, *64*, 3377–3405.

Orville, R. E., E. J. Zipser, M. Brook, C. Weidman, G. Aulich, E. P. Krider, H. Christian, S. Goodman, R. Blakeslee, and K. Cummins (1997), Lightning in the region of the TOGA COARE, *Bull. Am. Meteorol. Soc.*, *78*, 1055–1067.

Petersen, W. A., S. A. Rutledge, R. C. Cifelli, B. S. Ferrier, and B. F. Smull (1999), Shipborn Dual-Doppler operations during TOGA COARE: Integrated observations of storm kinematics and electrification, *Bull. Am. Meteorol. Soc.*, *80*, 81–97.

Price, C., M. Asfur, and Y. Yair (2009), Maximum hurricane intensity preceded by increase in lightning frequency, *Nat. Geosci.*, *2*, 329–332.

Rison, W., R. J. Thomas, P. R. Krehbiel, T. Hamlin, and J. Harlin (1999), A GPS-based three-dimensional lightning mapping system: Initial observations in Central New Mexico, *Geophys. Res. Lett.*, *26*, 3573–3576.

Rodger, C. J., J. B. Brundell, R. H. Holzworth, and E. H. Lay (2009), Growing detection efficiency of the World Wide Lightning Location Network, in *Am. Inst. Phys. Conf. Proc., Coupling of Thunderstorms and Lightning Discharges to Near-Earth Space: Proceedings of the Workshop, Corte (France), 23-–27 June 2008,* vol. 1118, edited by N. Crosby, T.-Y. Huang, and M. J. Rycroft, pp. 15–20, Am. Inst. of Phys., New York, doi:10.1063/1.3137706.

Rogers, R. (2010), Convective-scale structure and evolution during a high-resolution simulation of tropical cyclone rapid intensification., *J. Atmos. Sci.*, *67*, 44–69.

Samsury, C. E., and R. E. Orville (1994), Cloud-to-ground lightning in tropical cyclones: A study of hurricanes Hugo (1998) and Jerry (1989), *Mon. Weather Rev.*, *122*, 1887–1896.

Saunders, C. P. R., and S. L. Peck (1998), Laboratory studies of the influence of the rime accretion rate on charge transfer during crystal/graupel collisions, *J. Geophys. Res.*, *103*, 13,949–13,956.

Shao, X.-M., J. Harlin, M. Stock, M. Stanley, A. Regan, K. Wiens, T. Hamlin, M. Pongratz, D. Suszcynsky, and T. Light (2005), Katrina and Rita were lit up with lightning, *Eos, Trans. AGU*, *86*, 398–398, doi:10.1029/2005EO420004.

Shao, X.-M., M. Stanley, A. Regan, J. Harlin, M. Pongratz, and M. Stock (2006), Total lightning observations with the new and improved Los Alamos Sferic Array (LASA), *J. Atmos. Oceanic Technol.*, *23*, 1273–1288.

Shapiro, L. J. (1983), Asymmetric boundary layer flow under a translating hurricane, *J. Atmos. Sci.*, *40*, 1984–1998.

Soula, S., O. van der Velde, J. Montanya, P. Huet, C. Barthe, and J. Bór (2011), Gigantic jets produced by an isolated tropical thunderstorm near Réunion Island, *J. Geophys. Res.*, *116*, D19103, doi:10.1029/2010JD015581.

Squires, K., and S. Businger (2008), The morphology of eyewall lightning outbreak in two category 5 hurricanes, *Mon. Weather Rev.*, *136*, 1706–1726.

Takahashi, T. (1978), Riming electrification as a charge generation mechanism in thunderstorms, *J. Atmos. Sci.*, *35*, 1536–1548.

Thomas, R., P. Krehbiel, W. Rison, S. Hunyady, W. Winn, T. Hamlin, and J. Harlin (2004), Accuracy of the lightning mapping array, *J. Geophys. Res.*, *109*, D14207, doi:10.1029/2004JD004549.

Tuleya, R. E., and Y. Kurihara (1978), A numerical simulation of the landfall of tropical cyclones, *J. Atmos. Sci.*, *35*, 242–257.

Zhang, W., Y. Zhang, D. Zheng, and X. Zhou (2012), Lightning distribution and eyewall outbreaks in tropical cyclones during landfall, *Mon. Weather Rev.*, *140*, 3573–3586.